Xu et al. Chemistry Central Journal (2017) 11:20
DOI 10.1186/s13065-017-0250-z

Chemistry Central Journal

RESEARCH ARTICLE Open Access

Synthesis and protective effect of new ligustrazine-vanillic acid derivatives against $CoCl_2$-induced neurotoxicity in differentiated PC12 cells

Bing Xu[1], Xin Xu[1], Chenze Zhang[1], Yuzhong Zhang[2], GaoRong Wu[1], Mengmeng Yan[1], Menglu Jia[1], Tianxin Xie[1], Xiaohui Jia[1], Penglong Wang[1*] and Haimin Lei[1*]

Abstract

Ligustrazine-vanillic acid derivatives had been reported to exhibit promising neuroprotective activities. In our continuous effort to develop new ligustrazine derivatives with neuroprotective effects, we attempted the synthesis of several ligustrazine-vanillic acid amide derivatives and screened their protective effect on the injured PC12 cells damaged by $CoCl_2$. The results showed that most of the newly synthesized derivatives exhibited higher activity than ligustrazine, of which, compound **VA-06** displayed the highest potency with EC_{50} values of 17.39 ± 1.34 μM. Structure-activity relationships were briefly discussed.

Keywords: T-VA amide derivatives, Neuroprotective effect, Synthesis, PC12 cell

Background

Ischemic stroke is one of the leading causes of death and disability in the world [1–3]. It is clear that even a brief ischemic stroke may trigger complex cellular events that ultimately lead to the neuronal cell death and loss of neuronal function [1, 4, 5]. Although remarkable progress has been made in treating stroke, effective approaches to recover damaged nerve are not yet to be found [6–9]. Therefore, it is necessary to develop new generation of neuroprotective agents with neural repair-promoting effect.

Ligustrazine (tetramethylpyrazine, TMP) (Fig. 1) is a major effective component of the traditional Chinese medicine *Chuanxiong* (*Ligusticum chuanxiong hort*), which is currently widely used in clinic for the treatment of stroke in China. It has been reported to show beneficial effect on ischemic brain injury in animal experiments and in clinical practice [10–14].

Meanwhile previous studies showed that many of aromatic acids, such as vanillic acid, protocatechuic acid, salicylic acid, exhibited interesting neuroprotective activity [15–19]. In our previous effort to develop new neuroprotective lead compounds, inspired by the potent bioactivities of TMP and aromatic acids on neuroprotection, we designed and synthesized several series of ligustrazine derivatives by incorporation of ligustrazine with aromatic acids. The neuroprotective activity detection revealed that some compounds presented potent protective effects on injured differentiated PC12 cells, of which **T-VA** (3,5,6-trimethylpyrazin-2-yl)methyl3-methoxy-4-((3,5,6-trimethylpyrazin-2-yl)methoxy)benzoate) (Fig. 1) exhibited high potency with EC_{50} values of 4.249 μM [20–22]. Meanwhile, recent research has demonstrated that **T-VA** exerted neuroprotective in a rat model of ischemic stroke [23].

In continuation of our research, we decided to undertake a study of the ligustrazinyl amides, because amides relatively have metabolic stability when compared to ligustrazinyl esters [24]. In this study, we reported the design, synthesis of the novel T-VA amide analogues containing different types of amide fragments, as well

*Correspondence: wpl581@126.com; hm_lei@126.com
[1] School of Chinese Pharmacy, Beijing University of Chinese Medicine, Beijing 100102, China
Full list of author information is available at the end of the article

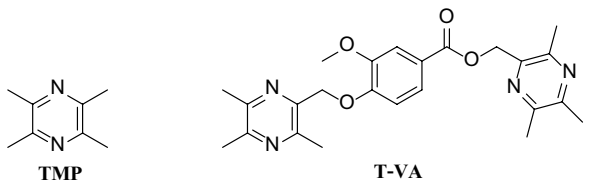

Fig. 1 Structures of TMP and T-VA

as in vitro neuroprotective activities screening on the injured PC12 cells. And the structure-activity relationships (SARs) of these novel compounds were also briefly discussed.

Results and discussion

Chemistry

All the target compounds were synthesized via the routes outlined in Scheme 1. The key intermediate (3,5,6-trimethylpyrazin-2-yl)methanol (**1**) was prepared according to our previous study [25]. As shown in Scheme 1, compound **1** underwent sulfonylation reaction with 4-toluene sulfonyl chloride to afford the intermediate **2**. Starting from vanillic acid, the intermediate **3** was prepared by reacting vanillic acid with methyl alcohol and thionyl chloride. Then the intermediate **3** were reacted with the intermediate **2** in N,N-Dimethylformamide (DMF) in the presence of potassium carbonate to afford the compound **VA-01**, which was then hydrolyzed under alkaline conditions to give the target compound **VA-02**.

The derivatives **VA-03–VA-23** were successfully obtained by coupling **VA-02** with various amines in the presence of 1-[3-(dimethylamino) propyl]-3-ethyl-carbodiimide hydrochloride (EDCI), diisopropylethylamine (DIPEA) and 1-hydroxybenzotriazole (HOBt) in CH_2Cl_2. The structures of all the target compounds (Table 1) were confirmed by spectral (^{1}H-NMR, ^{13}C-NMR) analysis and high resolution mass spectrometry (HRMS).

Protective effect on injured PC12 Cells

Setting ligustrazine and **T-VA** as the positive control drug, the neuroprotective activity of target compounds was evaluated on the neuronal-like PC12 cells damaged by $CoCl_2$. The results, expressed as proliferation rate (%) at different concentration and EC_{50}, were summarized in Table 2. As shown in Table 2, most of the ligustrazine-vanillic acid amide derivatives showed better protective effects than the positive control drug **TMP** ($EC_{50} = 64.35 \pm 1.47$ μM) on injured differentiated PC12 cells. Among the candidates, the compound **VA-06**

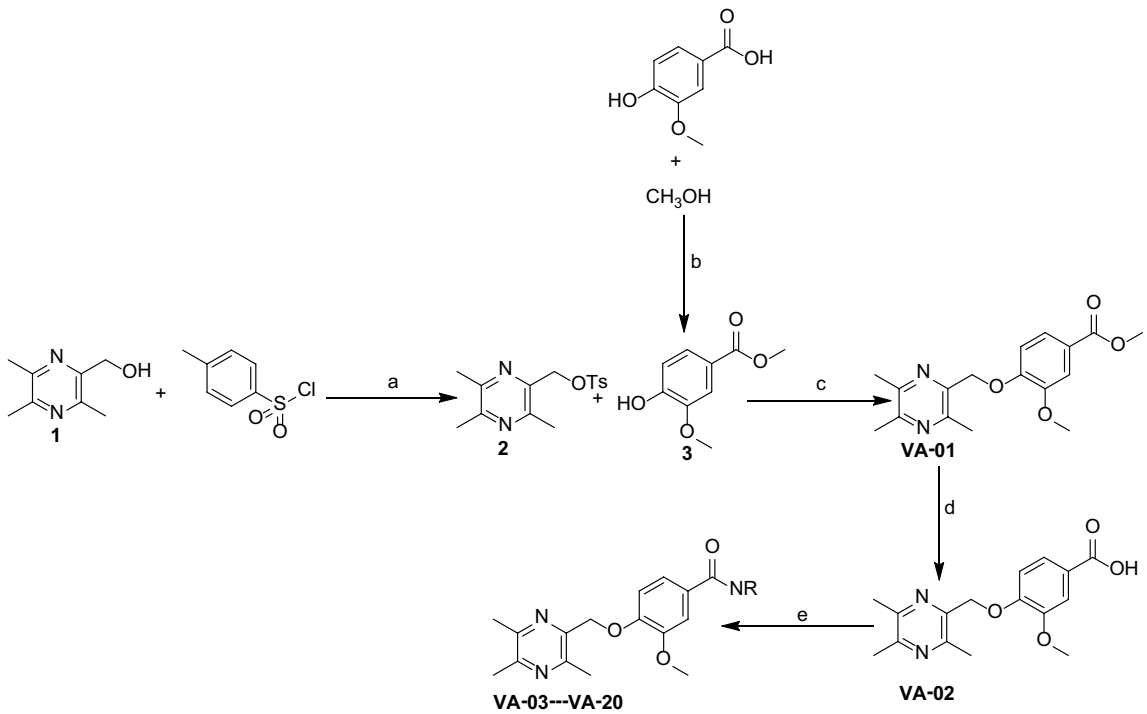

Scheme 1 Synthesis of the ligustrazine-vanillic acid derivative **VA-01**–**VA-20**. Reagents and Conditions: **a** dry THF, KOH, 4-toluene sulfonyl chloride (Tscl), 25 °C, 15 h; **b** thionyl chloride ($SOCl_2$), 25 °C, 15 h; **c** DMF, dry K_2CO_3, N_2, 70 °C, 15 h; **d** THF:MeOH:H_2O = 3:1:1, LiOH, 37 °C, 2 h; **e** DCM, HoBt, EDCI, DIPEA, 25 °C, 12 h

Table 1 The structures of ligustrazine derivatives VA-01–VA-20

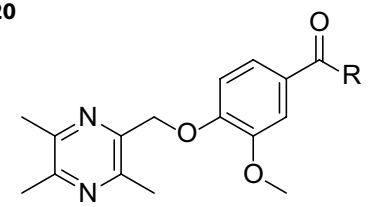

Compound	R	Yield (%)
VA-01	CH_3O–	52.5
VA-02	OH–	98.1
VA-03	CH_3CH_2NH–	89.5
VA-04		65.2
VA-05	CH_3NH–	87.0
VA-06	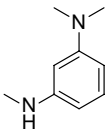	74.0
VA-07	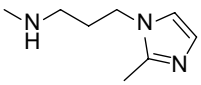	68.9
VA-08	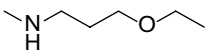	76.4
VA-09	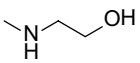	86.7
VA-10	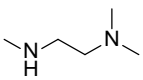	79.3
VA-11	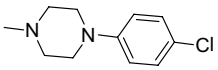	68.3
VA-12	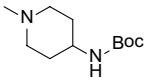	57.6
VA-13	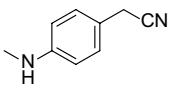	65.7
VA-14	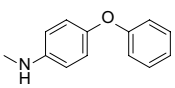	57.8
VA-15	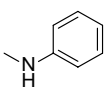	68.9
VA-16	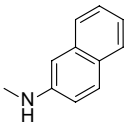	67.0
VA-17	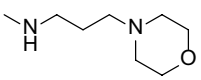	65.2

Table 1 continued

Compound	R	Yield (%)
VA-18	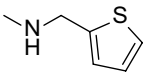	62.7
VA-19	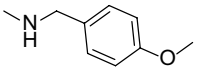	75.1
VA-20	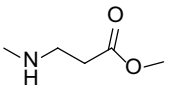	83.2

exhibited the most potent neuroprotective activity with EC_{50} values of 17.39 ± 1.34 μM.

From the obtained results, it was observed that esterification at the carboxylic group of vanillic acid may contribute to enhance the neuroprotective activity, such as **VA-01** > **VA-02**. This was in agreement with our previous research [20]. It should be noticed that introduction of a large lipophilic aromatic amine residue leaded to complete loss of neuroprotective activity (with exception of **VA-06**), such as **VA-13**–**VA-16**. But the compounds that introduced an aromatic amine residue at the carboxylic group of vanillic acid performed better neuroprotective activities than **VA-02** without any group substituted, such as **VA-03**, **VA-04**, **VA-05**, **VA-08** > **VA-02.** Furthermore, the structure-activity relationship analysis among the **T-VA** aromatic amide derivatives revealed that the neuroprotective activities were mainly influenced by the type, but not the alkyl chain length of amine substituents, as exemplify by **VA-04** > **VA-03**, **VA-05**. Although none of the newly synthesized T-VA derivatives showed more effect than the positive control drug **T-VA**, the structure-activity relationship (SAR) analysis above provided important information for further design of new neuroprotective ligustrazine derivatives.

Protective effect of VA-06 on injured PC12 cells

To further characterize the protective effect of **VA-06** on injured PC12 cells, the cell morphology changes were observed under an optical microscopy. As shown in Fig. 2, the morphology of undifferentiated PC12 cells was normal, the cells were small and proliferated to form clone-like cell clusters without neural characteristics (Fig. 2A); By exposure to NGF, normal differentiated PC12 cells showed round cell bodies with fine dendritic networks similar to those nerve cells (Fig. 2B). Moreover, the mean value expressed as percent of neurite-bearing cells in NGF treated cells was 65.4% (Fig. 3). When the differentiated PC12 cells treated with 250 mM $CoCl_2$ for 12 h, almost all cells showed typical morphological

Table 2 The EC_{50} of the ligustrazine-vanillic acid amide derivatives for protecting damaged PC12 cells

Compd	Proliferation rate (%)					EC_{50} (μM)[a]
	60 μM	30 μM	15 μM	7.5 μM	3.75 μM	
VA-01	81.75 ± 2.34	49.05 ± 4.07	43.15 ± 3.11	21.25 ± 1.25	22.77 ± 7.27	18.74 ± 1.94
VA-02	7.38 ± 0.95	12.55 ± 1.50	−0.47 ± 1.97	−11.43 ± 2.05	−10.48 ± 1.68	>100
VA-03	25.50 ± 1.48	21.42 ± 1.35	18.63 ± 0.82	13.34 ± 1.68	7.36 ± 1.73	52.48 ± 2.0
VA-04	46.60 ± 2.14	40.99 ± 3.08	41.49 ± 2.89	23.64 ± 2.32	6.88 ± 1.89	29.61 ± 0.78
VA-05	37.17 ± 2.17	31.36 ± 3.78	25.65 ± 2.05	21.54 ± 2.19	17.11 ± 1.51	36.61 ± 1.97
VA-06	89.81 ± 3.02	51.80 ± 5.61	29.51 ± 4.15	17.32 ± 6.10	15.78 ± 3.01	17.39 ± 1.34
VA-07	8.79 ± 2.27	53.07 ± 2.41	47.15 ± 1.31	7.42 ± 1.00	−5.52 ± 2.14	60.20 ± 25.70
VA-08	52.64 ± 2.94	29.29 ± 2.93	23.41 ± 1.71	18.50 ± 3.61	26.69 ± 5.58	33.62 ± 3.96
VA-09	49.34 ± 1.80	41.80 ± 0.81	41.56 ± 1.51	23.14 ± 2.78	14.05 ± 3.78	27.90 ± 1.65
VA-10	16.33 ± 1.60	33.99 ± 2.61	12.56 ± 4.21	15.66 ± 4.06	15.60 ± 5.67	48.79 ± 3.76
VA-11	32.99 ± 2.82	23.38 ± 2.92	15.20 ± 2.54	11.09 ± 0.67	14.44 ± 4.85	47.85 ± 1.84
VA-12	−71.58 ± 2.70	−59.50 ± 3.91	−35.73 ± 3.44	−11.99 ± 4.56	13.86 ± 2.28	>100
VA-13	−277.39 ± 4.12	−292.67 ± 10.71	−297.34 ± 12.0	−298.64 ± 8.39	−296.33 ± 11.32	>100
VA-14	15.86 ± 1.47	12.13 ± 1.17	8.64 ± 0.83	5.51 ± 0.69	2.69 ± 0.72	71.66 ± 2.12
VA-15	−198.39 ± 4.52	−60.74 ± 3.21	88.57 ± 7.11	48.83 ± 5.28	45.01 ± 8.01	>100
VA-16	−23.15 ± 3.05	−13.96 ± 1.49	−14.86 ± 2.64	−14.51 ± 1.40	2.99 ± 1.08	>100
VA-17	69.41 ± 4.00	52.29 ± 3.05	32.78 ± 0.96	18.63 ± 0.81	10.12 ± 0.59	24.73 ± 1.37
VA-18	5.32 ± 1.11	12.04 ± 0.44	15.96 ± 1.05	15.27 ± 0.74	−2.97 ± 0.85	71.92 ± 1.07
VA-19	15.21 ± 3.12	13.89 ± 2.96	8.23 ± 1.31	8.61 ± 1.45	10.52 ± 2.03	65.72 ± 2.93
VA-20	25.14 ± 4.22	17.38 ± 0.21	15.87 ± 1.05	15.12 ± 0.65	8.97 ± 0.49	53.74 ± 1.69
TMP	14.44 ± 0.76	12.24 ± 0.66	11.82 ± 0.45	10.80 ± 0.43	9.65 ± 0.71	64.35 ± 1.47
T-VA	127.27 ± 3.70	118.60 ± 7.47	88.59 ± 2.28	51.49 ± 1.14	31.01 ± 0.94	4.29 ± 0.47

[a] Mean value ± standard deviation from three independent experiments

changes such as cell body shrinkage and the disruption of the dendritic networks (Fig. 2C); the mean value of neurite-bearing cells (9.4%, Fig. 3) showed a significant decrease. While pretreatment with 60 μM **VA-06** before delivery of $CoCl_2$ dramatically alleviated the damage caused by $CoCl_2$ to cell morphology (Fig. 2D) and showed significant difference in the number of neurite-bearing cells (47.5%, Fig. 3) from that of $CoCl_2$ treatment alone.

Conclusions

In this study, we successfully synthesized 20 novel **T-VA** amide derivatives by combining **T-VA** with different amines. Their protective effects against $CoCl_2$-induced neurotoxicity in differentiated PC12 cells were determined by the MTT assay. The result indicated that most of **T-VA** amide derivatives showed protective effects on injured differentiated PC12 cells. Among them, a large portion of the derivatives were more active (with lower EC_{50} values) than the positive control drug **TMP**, of which compound **VA-06** displayed the highest neuroprotective effect with EC_{50} values of 17.39 ± 1.34 μM. Although none of the newly synthesized T-VA derivatives showed more effect than the positive control drug **T-VA**, the results enriched the study of ligustrazine derivatives with neuroprotective activity. Further bioassay of compound **VA-06** on neuroprotective activity on animal models is underway.

Methods

Chemistry

Reagents were bought from commercial suppliers without any further purification. Melting points were measured at a rate of 5 °C/min using an X-5 micro melting point apparatus (Beijing, China) and were not corrected. Reactions were monitored by TLC using silica gel coated aluminum sheets (Qingdao Haiyang Chemical Co., Qingdao, China). NMR spectra were recorded on a BRUKER AVANCE 500 NMR spectrometer (Fällanden, Switzerland) with tetramethylsilane (TMS) as an internal standard; chemical shifts δ were given in ppm and coupling constants J in Hz. HR-MS were acquired using a Thermo Sientific TM LTQ Orbitrap XL hybrid FTMS instrument (Thermo Technologies, New York, NY, USA). Cellular

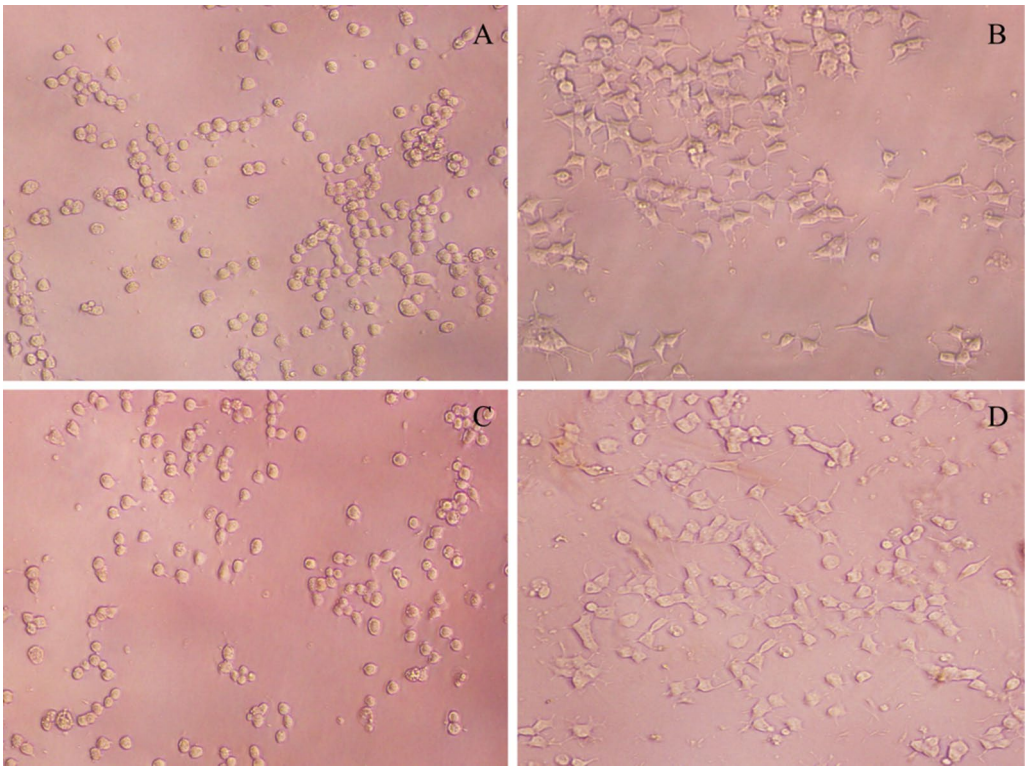

Fig. 2 Protective effects of compound **VA-06** against $CoCl_2$-induced injury in differentiated PC12 cells (×200) The most representative fields are shown. **A** Undifferentiated PC12 cells. **B** Differentiated PC12 cells by NGF. **C** $CoCl_2$-induced neurotoxicity of differentiated PC12 cells. **D** $CoCl_2$-induced neurotoxicity +**VA-06** (60 μM)

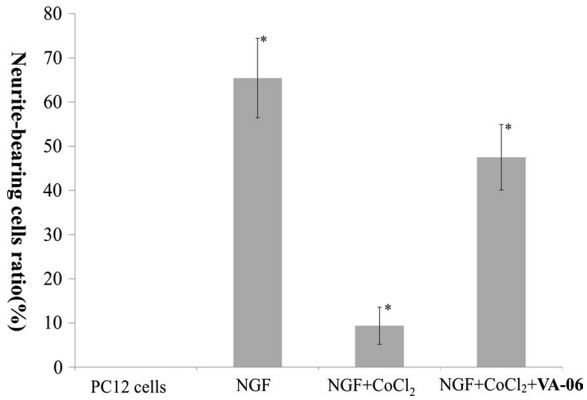

Fig. 3 Protective effects of compound **VA-06** (60 μM) against $CoCl_2$-induced injury in differentiated PC12 cells The neurite-bearing ration was shown as mean ± SD of at least 3 independent experiments. *$p \leq 0.05$ level, significance relative to $CoCl_2$ group

morphologies were observed using an inverted fluorescence microscope (Olympus IX71, Tokyo, Japan).

Synthesis of (3,5,6-trimethylpyrazin-2-yl)methanol (1)

Compound **1** was prepared according to our previously reported method [21].

Synthesis of (3,5,6-trimethylpyrazin-2-yl)methyl 4-methylbenzenesulfonate (2)

To a solution of compound **1** (7.0 g, 46.3 mmol) and KOH (2.6 g, 46.3 mmol) in dry THF (100 ml), Tscl (8.82 g, 46.3 mmol) was added, then the mixture was stirred at 25 °C for 15 h. After completion of the reaction (as monitored by TLC), the reaction mixture was poured into water and the crude product was extracted with dichloromethane (3 × 100 ml), the combined organic layers were washed with brine (100 ml), anhydrous Na_2SO_4, filtered and the solvents were evaporated under vacuum. The crude products were purified by flash chromatography (Petroleum ether:Ethyl acetate = 4:1) to produce a white solid. The crude product, with 90% purity, was not purified further.

Synthesis of methyl 4-hydroxy-3-methoxybenzoate (3)

To a solution of vanillic acid (5.502 g, 32.7 mmol) in dry MeOH (100 ml), 3 ml $SOCl_2$ was added gradually with stirring and cooling. Upon completion of the addition, the mixture was stirred at 25 °C for 15 h. After completion of the reaction (as monitored by TLC), the reaction mixture was evaporated under vacuum to produce a white solid. The crude product, with 95% purity, was not purified further.

Synthesis of methyl 3-methoxy-4-[(3,5,6-trimethylpyrazin-2-yl)methoxy] benzoate (VA-01)

Compound **2** (7.828 g, 256 mmol) and Compound **3** (3.580 g, 197 mmol) were dissolved in dry DMF, then K_2CO_3 (5.423 g, 393 mmol) was added and the mixture was kept at 70 °C for 15 h under nitrogen atmosphere. After completion of the reaction (as monitored by TLC), the reaction mixture was poured into ice-water and the crude product was extracted with dichloromethane. After drying the organic layer over anhydrous Na_2SO_4 and evaporating the solvent under vacuum, the crude products were purified by flash chromatography (Dichloromethane: methyl alcohol = 40:1) to produce a white solid.

*methyl 3-methoxy-4-[(3,5,6-trimethylpyrazin-2-yl)methoxy] benzoate (**VA-01**)* White solid, yield: 52.5%, m.p.: 140.0–140.7 °C. ^{1}H-NMR ($CDCl_3$) (ppm): 2.51 (s, 3H, $-CH_3$), 2.52 (s, 3H, $-CH_3$), 2.62 (s, 3H, $-CH_3$), 3.88 (s, 6H, 2× $-OCH_3$), 5.26 (s, 2H, $-CH_2$), 7.06 (d, J = 8.4 Hz, 1H, Ar–H), 7.53 (d, J = 1.2 Hz, 1H, Ar–H), 7.63 (dd, J = 1.2, 8.4 Hz, 1H, Ar–H). ^{13}C-NMR ($CDCl_3$) (ppm): 20.67 ($-CH_3$), 21.51 ($-CH_3$), 21.70 ($-CH_3$), 52.16 ($-OCH_3$), 56.12 ($-OCH_3$), 70.81 ($-CH_2$), 112.51, 112.82, 114.38, 123.41, 145.41, 148.91, 149.30, 150.12, 151.39, 151.99, 166.95 (–COO–). HRMS (ESI) m/z: 317.14905–3.4 ppm $[M+H]^+$, calcd. for $C_{17}H_{20}N_2O_4$ 316.14231.

Synthesis of 3-Methoxy-4-[(3,5,6-trimethylpyrazin-2-yl) methoxy]benzoic acid (VA-02)

An aqueous solution of LiOH (1.289 g, 307 mmol) was added to a solution of **VA-01** (3.237 g, 102 mmol) in THF:MeOH:H_2O = 3:1:1 (100 ml). The mixture was stirred at 37 °C for 2 h (checked by TLC). Upon completion of the reaction, pH was adjusted to 4–5 with 1 mol/l HCl. Then the reaction mixture was filtered and washed with water to give a white solid. The compound **VA-02** has been reported by us previously [20].

General procedure for the preparation of ligustrazine-vanillic acid derivative VA-03–VA-20

Compound **VA-02** (0.662 mmol, 1.0 eq) and the corresponding amine (0.926 mmol, 1.4 eq) were dissolved in 25 ml dry CH_2Cl_2, then HoBt (1.0592 mmol, 1.6 eq), EDCI (1.0592 mmol, 1.6 eq), DIPEA (1.986 mmol, 3.0 eq) were added and the mixture was kept at 25 °C for 12 h. After completion of the reaction (as monitored by TLC), the reaction mixture was poured into water and the crude product was extracted with dichloromethane (3 × 25 ml), the combined organic layers were washed with brine (50 ml), anhydrous Na_2SO_4, filtered and the solvents were evaporated under vacuum. The crude products were purified by flash chromatography (Petroleum ether:acetone = 5:1).

*N-ethyl-3-methoxy-4-((3,5,6-trimethylpyrazin-2-yl) methoxy)benzamide (**VA-03**)* White solid, yield: 89.5%, m.p.: 194.5–195.8 °C. ^{1}H-NMR ($CDCl_3$) (ppm): 1.22 (t, 3H, $-CH_3$), 2.49 (s, 3H, $-CH_3$), 2.50 (s, 3H, $-CH_3$), 2.60 (s, 3H, $-CH_3$), 3.45 (m, 2H, $-CH_2$), 3.86 (s, 3H, $-OCH_3$), 5.22 (s, 2H, $-CH_2$), 6.15 (s, 1H, –NH), 7.01 (d, J = 8.3 Hz, 1H, Ar–H), 7.21 (d, J = 8.3 Hz, 1H, Ar–H), 7.40 (s, 1H, Ar–H). ^{13}C-NMR ($CDCl_3$) (ppm): 15.06 ($-CH_3$), 20.65 ($-CH_3$), 21.48 ($-CH_3$), 21.68 ($-CH_3$), 35.03 ($-CH_2$), 56.11 ($-OCH_3$), 70.89 ($-CH_2$), 111.12, 113.09, 118.99, 128.30, 145.49, 148.81, 149.73, 150.13, 150.55, 151.33, 167.04 (–CONH–). HRMS (ESI) m/z: 330.18045–3.9 ppm $[M+H]^+$, calcd. for $C_{18}H_{23}N_3O_3$ 329.17394.

*(3-methoxy-4-((3,5,6-trimethylpyrazin-2-yl)methoxy)phenyl)(piperidin-1-yl)methanone (**VA-04**)* White solid, yield: 65.2%, m.p.: 176.0–176.8 °C. ^{1}H-NMR ($CDCl_3$) (ppm): 1.66 (m, 6H, 3× $-CH_2$), 2.50 (s, 3H, $-CH_3$), 2.51 (s, 3H, $-CH_3$), 2.61 (s, 3H, $-CH_3$), 3.39 (brs, 2H, $-CH_2$), 3.70 (m, 2H, $-CH_2$), 3.84 (s, 3H, $-OCH_3$) 5.21 (s, 2H, $-CH_2$), 6.90 (d, J = 8.1 Hz, 1H, Ar–H), 6.96 (s, 1H, Ar–H), 7.01 (d, J = 8.1 Hz, 1H, Ar–H), ^{13}C-NMR ($CDCl_3$) (ppm): 20.70 ($-CH_3$), 21.51 ($-CH_3$), 21.73 ($-CH_3$), 24.73, 31.11, 56.03 ($-OCH_3$), 58.48, 71.00 ($-CH_2$), 111.06, 113.45, 119.61, 129.68, 145.62, 148.75, 148.92, 149.65, 150.20, 151.30, 170.21 (–CON–). HRMS (ESI) m/z: 370.21179–3.4 ppm $[M+H]^+$, calcd. for $C_{21}H_{27}N_3O_3$ 369.20524.

*3-methoxy-N-methyl-4-((3,5,6-trimethylpyrazin-2-yl) methoxy)benzamide (**VA-05**)* White solid, yield: 87.0%, m.p.:173.5–174.5 °C. ^{1}H-NMR ($CDCl_3$) (ppm): 2.50 (s, 3H, $-CH_3$), 2.51 (s, 3H, $-CH_3$), 2.61 (s, 3H, $-CH_3$), 2.98 (s, 3H, $-CH_3$), 3.86 (s, 3H, $-OCH_3$), 5.23 (s, 2H, $-CH_2$), 6.20 (s, 1H, –NH), 7.02 (d, J = 8.0 Hz, 1H, Ar–H), 7.21 (d, J = 8.0 Hz, 1H, Ar–H), 7.40 (s, 1H, Ar–H). ^{13}C-NMR ($CDCl_3$) (ppm): 20.68 ($-CH_3$), 21.49 ($-CH_3$), 21.71 ($-CH_3$), 26.97 ($-CH_3$), 56.11 ($-OCH_3$), 70.90 ($-CH_2$), 111.08, 113.12, 119.06, 128.16, 145.48, 148.83, 149.73, 150.15, 150.60, 151.37, 167.87 (–CONH–). HRMS (ESI) m/z: 316.16489–3.9 ppm $[M+H]^+$, calcd. for $C_{17}H_{21}N_3O_3$ 315.15829.

*N-(3-(dimethylamino)phenyl)-3-methoxy-4-((3,5,6-trimethylpyrazin-2-yl)methoxy)benzamide (**VA-06**)* White solid, yield: 74.0%, m.p.: 171.4–172.3°C. ^{1}H-NMR ($CDCl_3$) (ppm): 2.51 (s, 6H, 2× $-CH_3$), 2.62 (s, 3H, $-CH_3$), 2.98 (s, 6H, 2× $-CH_3$), 3.91 (s, 3H, $-OCH_3$), 5.27 (s, 2H, $-CH_2$), 6.53 (d, J = 7.8 Hz, 1H, Ar–H), 6.81 (d, J = 7.8 Hz, 1H, Ar–H), 7.09 (d, J = 8.4 Hz, 1H, Ar–H), 7.20 (m, 1H, Ar–H), 7.33 (dd, J = 1.9 Hz, 8.4 Hz, 1H, Ar–H), 7.51

(d, J = 1.9 Hz, 1H, Ar–H), 7.69 (s, 1H, –NH). ^{13}C-NMR ($CDCl_3$) (ppm): 20.70 (–CH_3), 21.53 (–CH_3), 21.74 (–CH_3), 41.1 (–CH_3), 56.10 (–OCH_3), 70.74 (–CH_2), 103.80, 109.96, 111.25,111.40, 119.51, 120.83, 128.70, 129.82, 137.45, 145.34, 148.91, 149.22, 150.14, 151.45, 151.94, 152.52, 166.97 (–CON–). HRMS (ESI) m/z: 421.22144–6.0 ppm $[M+H]^+$, calcd. for $C_{24}H_{28}N_4O_3$ 420.21614.

*3-methoxy-N-(3-(2-methyl-1H-imidazol-1-yl) propyl)-4-((3,5,6-trimethylpyrazin-2-yl)methoxy)benzamide (**VA-07**)* White solid, yield: 68.9%, m.p.: 160.0–160.8 °C. ^{1}H-NMR ($CDCl_3$) (ppm): 2.04 (m, 2H, –CH_2), 2.35 (s, 3H, –CH_3), 2.48 (s, 3H, –CH_3), 2.49 (s, 3H, –CH_3), 2.59 (s, 3H, –CH_3), 3.45 (m, 2H, –CH_2), 3.86 (s, 3H, –OCH_3), 3.93 (m, 2H, –CH_2), 5.21 (s, 2H, –CH_2), 6.66 (m, 1H, –NH), 6.90 (s, 2H, 2× –CH), 7.02 (d, J = 8.4 Hz, 1H, Ar–H), 7.23 (d, J = 8.4 Hz, 1H, Ar–H), 7.40 (s, 1H, Ar–H). ^{13}C-NMR ($CDCl_3$) (ppm): 12.98 (–CH_3), 20.78 (–CH_3), 21.50 (–CH_3), 21.83 (–CH_3), 30.89 (–CH_2), 37.46 (–CH_2), 44.19 (–CH_2), 56.16 (–OCH_3), 70.91 (–CH_2), 111.08, 113.01, 119.37, 119.44, 126.73, 127.48, 144.46, 145.24, 148.70, 149.71, 150.24, 150.88, 151.55, 167.45 (–CONH–). HRMS (ESI) m/z: 424.23187–7.1 ppm $[M+H]^+$, calcd. for $C_{23}H_{29}N_5O_3$ 423.22704.

*N-(3-ethoxypropyl)-3-methoxy-4-((3,5,6-trimethylpyrazin-2-yl)methoxy)benzamide (**VA-08**)* White solid, yield: 76.4%, m.p.: 119.0–119.9 °C. ^{1}H-NMR ($CDCl_3$) (ppm): 1.23 (m, 3H, –CH_3), 1.88 (m, 2H, –CH_2), 2.50 (s, 3H, –CH_3), 2.51 (s, 3H, –CH_3), 2.61 (s, 3H, –CH_3), 3.50 (m, 2H, –CH_2), 3.55 (m, 2H, –CH_2), 3.61 (m, 2H, –CH_2), 3.88 (s, 3H, –OCH_3), 5.24 (s, 2H, –CH_2–), 7.03 (d, J = 8.3 Hz, 1H, Ar–H), 7.07 (s, 1H, –NH), 7.20 (d, J = 8.3 Hz, 1H, Ar–H), 7.42 (s, 1H, Ar–H). ^{13}C-NMR ($CDCl_3$) (ppm): 15.52 (–CH_3), 20.75 (–CH_3), 21.51 (–CH_3), 21.78 (–CH_3), 28.88 (–CH_2), 39.70, 56.11 (–OCH_3), 58.58, 66.73, 70.83 (–CH_2), 111.05, 112.97, 118.94, 128.32, 145.46, 148.75, 149.65, 150.24, 150.46, 151.41, 166.80 (–CONH–). HRMS (ESI) m/z: 388.22171–5.0 ppm $[M+H]^+$, calcd. for $C_{21}H_{29}N_3O_4$ 387.21581.

*N-(2-hydroxyethyl)-3-methoxy-4-((3,5,6-trimethylpyrazin-2-yl)methoxy)benzamide (**VA-09**)* Brick-red solid, yield: 86.7%, m.p.: 156.9–157.9 °C. ^{1}H-NMR ($CDCl_3$) (ppm): 2.50 (s, 3H, –CH_3), 2.51 (s, 3H, –CH_3), 2.61 (s, 3H, –CH_3), 3.59 (m, 2H, –CH_2), 3.81 (m, 2H, –CH_2), 3.87 (s, 3H, –OCH_3), 5.23 (s, 2H, –CH_2), 6.63 (s, 1H, –NH), 7.03 (d, J = 8.4 Hz, 1H, Ar–H), 7.25 (dd, J = 2.0, 8.4 Hz, 1H, Ar–H), 7.40 (d, J = 2.0 Hz, 1H, Ar–H). ^{13}C-NMR ($CDCl_3$) (ppm): 20.65 (–CH_3), 21.42 (–CH_3), 21.69 (–CH_3), 43.01 (–CH_2), 56.08 (–OCH_3), 62.27 (–CH_2), 70.71 (–CH_2), 111.07, 112.97, 119.50, 127.54, 145.25, 148.83, 149.61, 150.16, 150.80, 151.54, 168.15 (–CONH–). HRMS (ESI) m/z: 346.17517–4.4 ppm $[M+H]^+$, calcd. for $C_{18}H_{23}N_3O_4$ 345.16886.

*N-(2-(dimethylamino)ethyl)-3-methoxy-4-((3,5,6-trimethylpyrazin-2-yl)methoxy)benzamide (**VA-10**)* White solid, yield: 79.3%, m.p.: 148.6–149.0 °C. ^{1}H-NMR ($CDCl_3$) (ppm): 2.51 (s, 6H, 2× –CH_3), 2.52 (s, 2H, –CH_2), 2.54 (s, 6H, 2× –CH_3), 2.62 (s, 3H, –CH_3), 3.92 (s, 3H, –OCH_3), 4.65 (d, 2H, –CH_2), 5.26 (s, 2H, –CH_2–), 7.09 (d, J = 8.4 Hz, 1H, Ar–H), 7.38 (dd, J = 2.0, 8.4 Hz, 1H, Ar–H), 7.51 (d, J = 2.0 Hz, 1H, Ar–H), 7.82 (brs, 1H, –NH). ^{13}C-NMR ($CDCl_3$) (ppm): 20.75 (–CH_3), 21.48 (–CH_3), 21.79 (–CH_3), 27.41, 32.33, 51.08, 56.14 (–OCH_3), 70.92 (–CH_2), 111.35, 113.07, 118.72, 128.48, 145.34, 148.68, 149.82, 150.24, 150.64, 151.49, 167.32 (–CONH–). HRMS (ESI) m/z: 373.23010+16.4 ppm $[M+H]^+$, calcd. for $C_{20}H_{28}N_4O_3$ 372.21614.

*(4-(4-chlorophenyl)piperazin-1-yl)(3-methoxy-4-((3,5,6-trimethylpyrazin-2-yl)methoxy)phenyl) methanone (**VA-11**)* White solid, yield: 68.3%, m.p.: 179.0–179.5 °C. ^{1}H-NMR ($CDCl_3$) (ppm): 2.51 (s, 3H, –CH_3), 2.53 (s, 3H, –CH_3), 2.63 (s, 3H, –CH_3), 3.16 (brs, 4H, 2× –CH_2), 3.79 (brs, 4H, 2× –CH_2), 3.86 (s, 3H, –OCH_3), 5.24 (s, 2H, –CH_2), 6.87 (d, J = 8.2 Hz, 2H, Ar–H), 6.96 (d, J = 8.2 Hz, 1H, Ar–H), 7.01 (s, 1H, Ar–H), 7.05 (d, J = 8.2 Hz, 1H, Ar–H), 7.23 (d, J = 8.2 Hz, 2H, Ar–H). ^{13}C-NMR ($CDCl_3$) (ppm): 20.62 (–CH_3), 21.51 (–CH_3), 21.65 (–CH_3), 29.83, 32.08, 37.07, 49.99 (–CH_2), 56.15 (–OCH_3), 71.04 (–CH_2), 111.46, 113.53, 118.14, 120.08, 128.59, 129.30, 145.67, 148.90, 149.48, 149.90, 150.13, 151.29, 170.37 (–CON–). HRMS (ESI) m/z: 481.19775–6.0 ppm $[M+H]^+$, calcd. for $C_{26}H_{29}ClN_4O_3$ 480.19282.

*tert-butyl4-(3-methoxy-4-((3,5,6-trimethylpyrazin-2-yl)methoxy)benzoyl)piperazine-1-carboxylate (**VA-12**)* White solid, yield: 57.6%, m.p.: 86.6–87.6 °C. ^{1}H-NMR ($CDCl_3$) (ppm): 1.36 (brs, 2H, –CH_2), 1.44 (s, 9H, 3× –CH_3), 1.99 (brs, 2H, –CH_2), 2.50 (s, 3H, –CH_3), 2.52 (s, 3H, –CH_3), 2.62 (s, 3H, –CH_3), 3.02 (brs, 2H, –CH_2), 3.70 (brs, 2H, –CH_2), 3.84 (s, 3H, –OCH_3), 4.47 (brs, 2H, –CH_2), 5.22 (s, 2H, –CH_2–), 6.90 (dd, J = 1.6 Hz, 8.2 Hz, 1H, Ar–H), 6.96 (d, J = 1.6 Hz, 1H, Ar–H), 7.02 (d, J = 8.2 Hz, 1H, Ar–H). ^{13}C-NMR ($CDCl_3$) (ppm): 20.64 (–CH_3), 21.49 (–CH_3), 21.66 (–CH_3), 28.49 (–CH_3), 33.01, 41.35, 48.08 (–CH), 56.09 (–OCH_3), 71.03 (–CH_2), 79.75 (–OCH), 111.22, 113.55, 119.77, 129.10, 145.66, 148.83, 149.26, 149.79, 150.14, 151.26, 155.16 (–COO–), 170.35 (–CON–). HRMS (ESI) m/z: 485.27286–7.3 ppm $[M+H]^+$, calcd. for $C_{26}H_{36}N_4O_5$ 484.26857.

N-(4-(cyanomethyl)phenyl)-3-methoxy-4-((3,5,6-trimethylpyrazin-2-yl)methoxy)benzamide ***(VA-13)*** White solid, yield: 65.7%, m.p.:199.0–199.5 °C. ^{1}H-NMR ($CDCl_3$) (ppm): 2.51 (s, 3H, –CH_3), 2.52 (s, 3H, –CH_3), 2.62 (s, 3H, –CH_3), 3.74 (s, 2H, –CH_2), 3.90 (s, 3H, –OCH_3), 5.27 (s, 2H, –CH_2), 7.09 (d, J = 8.2 Hz, 1H, Ar–H), 7.32 (d, 2H, Ar–H) 7.35 (dd, J = 1.8, 8.2 Hz, 1H, Ar–H), 7.48 (s, 1H, Ar–H), 7.65 (d, J = 8.2 Hz, 2H, Ar–H), 7.87 (brs, 1H, –NH). ^{13}C-NMR ($CDCl_3$) (ppm): 20.66 (–CH_3), 21.47 (–CH_3), 21.70 (–CH_3), 23.24, 56.14 (–OCH_3), 70.80 (–CH_2), 111.24, 112.96, 118.09, 119.51, 120.83, 125.59, 127.96, 128.70, 138.15, 145.27, 148.92, 149.85, 150.11, 151.16, 151.51, 165.45 (–CON–). HRMS (ESI) m/z: 417.19052–5.2 ppm $[M+H]^+$, calcd. for $C_{24}H_{24}N_4O_3$ 416.18484.

3-methoxy-N-(4-phenoxyphenyl)-4-((3,5,6-trimethylpyrazin-2-yl)methoxy)benzamide ***(VA-14)*** White solid, yield: 57.8%, m.p.: 182.5–183.3 °C. ^{1}H-NMR ($CDCl_3$) (ppm): 2.52 (s, 3H, –CH_3), 2.53 (s, 3H, –CH_3), 2.64 (s, 3H, –CH_3), 3.91 (s, 3H, –OCH_3), 5.27 (s, 2H, –CH_2), 7.01 (m, 4H, Ar–H), 7.09 (m, 2H, Ar–H), 7.33 (m, 3H, Ar–H), 7.49 (d, J = 2 Hz, 1H, Ar–H), 7.58 (m, 2H, Ar–H), 7.78 (brs, 1H, –NH). ^{13}C-NMR ($CDCl_3$) (ppm): 20.63 (–CH_3), 21.50 (–CH_3), 21.66 (–CH_3), 56.16 (–OCH_3), 70.85 (–CH_2), 111.27, 113.07, 118.59, 120.04, 119.75, 122.04, 123.23, 128.25, 129.86, 133.66, 145.40, 148.96, 149.90, 150.09, 151.03, 151.42, 153.68, 157.62, 165.35 (–CON–). HRMS (ESI) m/z: 470.20447–7.5 ppm $[M+H]^+$, calcd. for $C_{28}H_{27}N_3O_4$ 469.20016.

3-methoxy-N-phenyl-4-((3,5,6-trimethylpyrazin-2-yl) methoxy)benzamide ***(VA-15)*** White solid, yield: 68.9%, m.p.: 189.7–190.2 °C. ^{1}H-NMR ($CDCl_3$) (ppm): 2.50 (s, 3H, –CH_3), 2.51 (s, 3H, –CH_3), 2.62 (s, 3H, –CH_3), 3.89 (s, 3H, –OCH_3), 5.26 (s, 2H, –CH_2–), 7.08 (d, J = 8.3 Hz, 1H, Ar–H), 7.14 (m, 1H, Ar–H), 7.35 (m, 3H, Ar–H), 7.49 (d, J = 1.8 Hz, 1H, Ar–H), 7.62 (d, 2H, Ar–H), 7.81 (s, 1H, –NH–). ^{13}C-NMR ($CDCl_3$) (ppm): 20.65 (–CH_3), 21.47 (–CH_3), 21.69 (–CH_3), 56.08 (–OCH_3), 70.81 (–CH_2), 111.25, 112.95, 119.39, 120.26, 124.46, 128.33, 129.12, 138.19, 145.29, 148.87, 149.81, 150.10, 150.99, 151.46, 165.42 (–CONH–). HRMS (ESI) m/z: 378.18002–4.6 ppm $[M+H]^+$, calcd. for $C_{22}H_{23}N_3O_3$ 377.17394.

3-methoxy-N-(naphthalen-2-yl)-4-((3,5,6-trimethylpyrazin-2-yl)methoxy)benzamide ***(VA-16)*** White solid, yield: 67.0%, m.p.: 174.1–175.0 °C.^{1}H-NMR ($CDCl_3$) (ppm): 2.53 (s, 6H, 2× –CH_3), 2.65 (s, 3H, –CH_3), 3.92 (s, 3H, –OCH_3), 5.30 (s, 2H, –CH_2), 7.14 (d, J = 8.2 Hz, 1H, Ar–H), 7.52 (m, 4H, Ar–H), 7.58 (s, 1H, Ar–H), 7.74 (d, J = 8.2 Hz, 1H, Ar–H), 7.90 (m, 2H, Ar–H), 7.99 (m, 1H, Ar–H), 8.17 (s, 1H, –NH–). ^{13}C-NMR ($CDCl_3$) (ppm): 20.66 (–CH_3), 21.49 (–CH_3), 21.66 (–CH_3), 56.16 (–OCH_3), 70.86 (–CH_2), 111.49, 113.05, 119.44, 121.03, 121.47, 125.88, 126.15, 126.43, 127.73, 128.19, 128.87, 132.70, 134.25, 145.39, 148.93, 149.94, 150.11, 151.11, 151.43, 166.02 (–CONH–). HRMS (ESI) m/z: 428.19547–4.6 ppm $[M+H]^+$, calcd. for $C_{26}H_{25}N_3O_3$ 427.18959.

3-methoxy-N-(3-morpholinopropyl)-4-((3,5,6-trimethylpyrazin-2-yl)methoxy)benzamide ***(VA-17)*** White solid, yield: 65.2%, m.p.: 129.2–129.5 °C. ^{1}H-NMR ($CDCl_3$) (ppm): 1.79 (m, 2H, –CH_2), 2.50 (m, 10H), 2.55 (m, 2H, –CH_2), 2.61 (s, 3H, –CH_3), 3.55 (m, 2H, –CH_2), 3.70 (m, 4H, 2× –CH_2), 3.89 (s, 3H, –OCH_3), 5.25 (s, 2H, –CH_2), 7.05 (d, J = 8.3 Hz, 1H, Ar–H), 7.24 (dd, J = 1.6, 8.3 Hz, 1H, Ar–H), 7.47 (d, J = 1.6 Hz, 1H, Ar–H), 7.75 (brs, 1H, –NH–). ^{13}C-NMR ($CDCl_3$) (ppm): 20.79 (–CH_3), 21.47 (–CH_3), 21.82 (–CH_3), 24.40, 40.42 (–CH_2), 53.86 (–CH_2), 56.19 (–OCH_3), 58.59, 66.90, 70.91 (–CH_2), 111.42, 112.94, 118.95, 128.28, 145.34, 148.67, 149.77, 150.26, 150.59, 151.47, 167.06 (–CONH–). HRMS (ESI) m/z: 429.24731–6.6 ppm $[M+H]^+$, calcd. for $C_{23}H_{32}N_4O_4$ 428.24232.

3-methoxy-N-(thiophen-2-ylmethyl)-4-((3,5,6-trimethylpyrazin-2-yl)methoxy)benzamide ***(VA-18)*** White solid, yield: 62.7%, m.p.:156.3–156.9 °C. ^{1}H-NMR ($CDCl_3$) (ppm): 2.50 (s, 3H, –CH_3), 2.52 (s, 3H, –CH_3), 2.62 (s, 3H, –CH_3), 3.89 (s, 3H, –OCH_3), 4.80 (d, 2H, –CH_2), 5.24 (s, 2H, –CH_2), 6.36 (brs, 1H, –NH), 6.97 (m, 1H, –CH), 7.03 (m, 2H, 2× –CH), 7.22 (dd, J = 2.0, 8.3 Hz, 1H, Ar–H), 7.24 (d, 1H, Ar–H), 7.44 (d, J = 2.0 Hz, 1H, Ar–H). ^{13}C-NMR ($CDCl_3$) (ppm): 20.42 (–CH_3), 21.47 (–CH_3), 29.84 (–CH_3), 38.97 (–CH_2), 56.18 (–OCH_3), 70.80 (–CH_2), 111.28, 113.13, 119.22, 125.50, 126.36, 127.09, 127.66, 141.03, 144.09, 145.78, 149.19, 149.83, 150.80, 151.46, 166.73 (–CONH–). HRMS (ESI) m/z: 398.15253–3.3 ppm $[M+H]^+$, calcd. for $C_{21}H_{23}N_3O_3$ S 397.14601.

3-methoxy-N-(4-methoxybenzyl)-4-((3,5,6-trimethylpyrazin-2-yl)methoxy)benzamide ***(VA-19)*** White solid, yield: 75.1%, m.p.: 161.6–162.3 °C. ^{1}H-NMR ($CDCl_3$) (ppm): 2.48 (s, 3H, –CH_3), 2.49 (s, 3H, –CH_3), 2.59 (s, 3H, –CH_3), 3.78 (s, 3H, –OCH_3), 3.86 (s, 3H, –OCH_3), 4.53 (d, 2H, –CH_2), 5.22 (s, 2H, –CH_2), 6.41 (s, 1H, –NH), 6.85 (s, 1 H, Ar–H), 6.86 (d, J = 8.0 Hz, 2 H, Ar–H), 7.00 (d, J = 8.3 Hz, 1 H, Ar–H), 7.19 (m, 1 H, Ar–H),, 7.25 (d, J = 8.0 Hz, 2 H, Ar–H), 7.43 (s, 1H, Ar–H). ^{13}C-NMR ($CDCl_3$) (ppm): 20.68 (–CH_3), 21.50 (–CH_3), 21.72 (–CH_3), 43.72 (–CH_2–), 55.2 (–OCH_3), 56.10 (–OCH_3), 70.81 (–CH_2), 111.12, 112.92, 114.17, 119.11, 127.79, 129.42, 130.44, 145.38, 148.79, 149.68, 150.15, 150.67, 151.41, 159.13, 166.87 (–CONH–). HRMS (ESI) m/z: 422.21408–14.0 ppm $[M+H]^+$, calcd. for $C_{24}H_{27}N_3O_4$ 421.20016.

*Methyl 3-(3-methoxy-4-((3,5,6-trimethylpyrazin-2-yl) methoxy)benzamido)propanoate (**VA-20**)* White solid, yield: 83.2%, m.p.: 139.6–140.1 °C. ^{1}H-NMR ($CDCl_3$) (ppm): 2.51 (s, 3H, $-CH_3$), 2.52 (s, 3H, $-CH_3$), 2.61 (s, 3H, $-CH_3$), 2.64 (t, 2H, $-CH_2$), 3.69 (m, 2H, $-CH_2$), 3.70 (s, 3H, $-OCH_3$), 3.88 (s, 3H, $-OCH_3$), 5.24 (s, 2H, $-CH_2$), 6.80 (s, 1H, –NH), 7.02 (d, J = 8.3 Hz, 1H, Ar–H), 7.20 (d, J = 8.3 Hz, 1H, Ar–H), 7.40 (s, 1H, Ar–H). ^{13}C-NMR ($CDCl_3$) (ppm): 20.59 ($-CH_3$), 21.52 ($-CH_3$), 21.63 ($-CH_3$), 33.82 ($-CH_2$), 35.36 ($-CH_2$), 52.02 ($-OCH_3$), 56.12 ($-OCH_3$), 70.80 ($-CH_2$), 111.06, 112.97, 119.15, 127.75, 145.56, 147.42, 149.67, 150.06, 150.66, 151.30, 166.97 (–CONH–), 173.61 (–COO–). HRMS (ESI) m/z: 388.18057–17 ppm [M+H]+, calcd. for $C_{20}H_{25}N_3O_5$ 387.17942.

Bio-evaluation methods

Cell culture

PC12 cells were obtained from the Chinese Academy of Medical Sciences & Peking Union Medical College. The cultures of the PC12 cells were maintained as monolayer in RPMI 1640 supplemented with 10% (v/v) heat inactivated (Gibco) horse serum, 5% (v/v) fetal bovine serum and 1% (v/v) penicillin/streptomycin (Thermo Technologies, New York, NY,USA) and incubated at 37 °C in a humidified atmosphere with 5% CO_2. **T-VA** amide derivatives were dissolved in dimethyl sulfoxide (DMSO).

Protective effect on damaged differentiated pc12 cells

The neuroprotective effect of newly synthesized **T-VA** amide derivatives was evaluated in vitro via the MTT method on the differentiated PC12 cells damaged by $CoCl_2$ with ligustrazine as the positive control. PC12 cells growing in the logarithmic phase were incubated in the culture dishe and allowed to grow to the desired confluence. Then the cells were switched to fresh serum-free medium and incubated for 14 h. At the end of this incubation, the PC12 cells were collected and resuspended in 1640 medium supplemented with 10% (v/v) fetal bovine serum, then the cells were seeded in poly-L-lysine-coated 96-well culture plates at a density of 7×10^3 cells/well and incubated for another 48 h in the presence of 50 ng/ml NGF.

The differentiated PC12 cells were pretreated with serial dilutions of **T-VA** amide derivatives (60, 30, 15, 7.5, 3.75 μM) for 36 h, and then exposed to $CoCl_2$ (final concentration, 250 mM) for another 12 h. Control differentiated cells were not treated with **T-VA** amide derivatives and $CoCl_2$. At the end of this incubation, 20 μl of 5 mg/ml methylthiazol tetrazolium (MTT) was added to each well and incubation proceeded at 37 °C for another 4 h. After the supernatant medium was removed carefully, 200 μl dimethylsulphoxide (DMSO) were added to each well and absorbance was measured at 490 nm using a plate reader (BIORAD 550 spectrophotometer, Bio-rad Life Science Development Ltd., Beijing, China). The proliferation rates of damaged PC12 cells were calculated by the formula $[OD_{490}(\text{Compd}) - OD_{490}(CoCl_2)]/[OD_{490}(\text{NGF}) - OD_{490}(CoCl_2)] \times 100\%$; The concentration of the compounds which produces a 50% proliferation of surviving cells corresponds to the EC_{50}. And it was calculated using the following equation: $-pEC_{50} = \log C_{max} - \log 2 \times (\sum P - 0.75 + 0.25P_{max} + 0.25P_{min})$, where C_{max} = maximum concentration, $\sum P$ = sum of proliferation rates, P_{max} = maximum value of proliferation rate and P_{min} = minimum value of proliferation rate [20–22].

Observation of morphologic changes

The changes in cell morphology after treatment with **VA-06** were determined using light microscopy in this assay, it was performed as previously described [22]. Differentiation was scored as the cells with one or more growth cone tipped neurites greater than 2 cell bodies in length. The cell differentiation rate was calculated by the formula [the number of differentiated cells]/[the number of total cells] × 100%. Three fields were randomly chosen from different wells of three independent experiments. All data are expressed as mean ± standard deviation (SD). Statistical analyses were performed using SAS version 9.0 (SAS Institute Inc., Cary, NC, USA). Between-groups differences were assessed using Student t tests and $p < 0.05$ was considered significant.

Authors' contributions

BX, PW and HL designed the study; BX, XX, CZ and GW carried out the chemistry and biology studies; MY, MJ, TX, XJ collected and analyzed data; BX and PW wrote the paper. All authors read and approved the final manuscript.

Author details

[1] School of Chinese Pharmacy, Beijing University of Chinese Medicine, Beijing 100102, China. [2] Department of Pathology, Beijing University of Chinese Medicine, Beijing 100102, China.

Acknowledgements

The authors acknowledge the financial support from National Natural Science Foundation of China (No. 81173519), Innovation Team Project Foundation of Beijing University of Chinese Medicine named 'Lead Compounds Discovering and Developing Innovation Team Project Foundation' (No. 2011-CXTD-15), Beijing Key Laboratory for Basic and Development Research on Chinese Medicine and young teachers' scientific research project of Beijing University of Chinese Medicine (No. 2015-JYB-JSMS023).

Competing interests

The authors declare that they have no competing interests.

Funding

The synthesis work was supported by the National Natural Science Foundation of China (No. 81173519) and Beijing Key Laboratory for Basic and Development Research on Chinese Medicine; The neurotoxicity evaluation work was supported by the Innovation Team Project Foundation of Beijing University of Chinese Medicine named 'Lead Compounds Discovering and Developing Innovation Team Project Foundation' (No. 2011-CXTD-15), The page charge was supported by young teachers' scientific research project of Beijing University of Chinese Medicine (No. 2015-JYB-JSMS023).

Received: 11 January 2017 Accepted: 21 February 2017
Published online: 28 February 2017

References

1. Deb P, Sharma S, Hassan KM (2010) Pathophysiologic mechanisms of acute ischemic stroke: an overview with emphasis on therapeutic significance beyond thrombolysis. Pathophysiology 17:197–218
2. Mang J, Mei CL, Wang JQ, Li ZS, Chu TT, He JT et al (2013) Endogenous protection derived from activin A/Smads transduction loop stimulated via ischemic injury in PC12 cells. Molecules 18:12977–12986
3. Williams LS, Ghose SS, Swindle RW (2004) Depression and other mental health diagnoses increase mortality risk after ischemic stroke. Am J Psychiatry 161:1090–1095
4. Yuan J (2009) Neuroprotective strategies targeting apoptotic and necrotic cell death for stroke. Apoptosis 14:469–477
5. Broughton BR, Reutens DC, Sobey CG (2009) Apoptotic mechanisms after cerebral ischemia. Stroke 40:331–339
6. Campbell BC, Mitchell PJ, Kleinig TJ, Dewey HM, Churilov L, Yassi N et al (2015) Endovascular therapy for ischemic stroke with perfusion-imaging selection. N Engl J Med 372:1009–1018
7. Misra V, Ritchie MM, Stone LL, Low WC, Janardhan V (2012) Stem cell therapy in ischemic stroke: role of IV and intra-arterial therapy. Neurology 79:207–212
8. Woodruff TM, Thundyil J, Tang SC, Sobey CG, Taylor SM, Arumugam TV et al (2011) Pathophysiology, treatment, and animal and cellular models of human ischemic stroke. Mol Neurodegener 6:1–19
9. Raghavan A, Shah ZA (2015) Withania somnifera improves ischemic stroke outcomes by attenuating PARP1-AIF-mediated caspase-independent apoptosis. Mol Neurobiol 52:1093–1105
10. Fan LH, Wang KZ, Shi ZB, Die J, Wang CS, Dang XQ (2011) Tetramethylpyrazine protects spinal cord and reduces inflammation in a rat model of spinal cord ischemia-reperfusion injury. J Vasc Surg 54:192–200
11. Kao TK, Chang CY, Ou YC, Chen WY, Kuan YH, Pan HC et al (2013) Tetramethylpyrazine reduces cellular inflammatory response following permanent focal cerebral ischemia in rats. Exp Neurol 247:188–201
12. Fan LH, Wang KZ, Cheng B, Wang CS, Dang XQ (2006) Anti-apoptotic and neuroprotective effects of tetramethylpyrazine following spinal cord ischemia in rabbits. BMC Neurosci 7:48
13. Chen L, Wei XB, Hou YF, Liu XQ, Li SP, Sun BZ et al (2014) Tetramethylpyrazine analogue CXC195 protects against cerebral ischemia/reperfusion-induced apoptosis through PI3 K/Akt/GSK3β pathway in rats. Neurochem Int 66:27–32
14. Sun YW, Yu P, Zhang GX, Wang L, Zhong HJ, Zhai ZY et al (2012) Therapeutic effects of tetramethylpyrazine nitrone in rat ischemic stroke models. J Neurosci Res 90:1662–1669
15. Zhang ZJ, Li GH, Szeto SSW, Chong MC, Quan Q, Huang C et al (2015) Examining the neuroprotective effects of protocatechuic acid and chrysin on in vitro and in vivo models of Parkinson disease. Free Radic Biol Med 84:331–343
16. Singh JCH, Kakalij RM, Kshirsagar RP, Kumar BH, Komakula SSB, Diwan PV et al (2015) Cognitive effects of vanillic acid against streptozotocin-induced neurodegeneration in mice. Pharm Biol 53:630–636
17. Amin FU, Shah SA, Kim MO (2017) Vanillic acid attenuates Aβ1-42-induced oxidative stress and cognitive impairment in mice. Sci Rep 7:40753
18. Thrash-Williams B, Karuppagounder SS, Bhattacharya D, Ahuja M, Suppiramaniam V, Dhanasekaran M (2016) Methamphetamine-induced dopaminergic toxicity prevented owing to the neuroprotective effects of salicylic acid. Life Sci 154:24–29
19. Cetin D, Hacımuftuoglu A, Tatar A, Turkez H, Togar B (2016) The in vitro protective effect of salicylic acid against paclitaxel and cisplatin-induced neurotoxicity. Cytotechnology 68:1361–1367
20. Wang PL, Zhang HG, Chu FH, Xu X, Lin JX, Chen CX et al (2013) Synthesis and protective effect of new ligustrazine-benzoic acid derivatives against $CoCl_2$-induced neurotoxicity in differentiated PC12 cells. Molecules 18:13027–13042
21. Li GL, Xu X, Xu K, Chu FH, Song JX, Zhou S et al (2015) Ligustrazinyl amides: a novel class of ligustrazine-phenolic acid derivatives with neuroprotective effects. Chem Cent J 9:9
22. Xu B, Gong Y, Xu X, Zhang CZ, Zhang YZ, Chu FH et al (2015) Synthesis and protective effect of new ligustrazine derivatives against $CoCl_2$-induced neurotoxicity in differentiated PC12 cells. Part 2. Med Chem Commun 6:806–809
23. Li GL, Tian YF, Zhang YZ, Hong Y, Hao YZ, Chen CX et al (2015) A novel ligustrazine derivative T-VA prevents neurotoxicity in differentiated PC12 cells and protects the brain against ischemia injury in MCAO rats. Int J Mol Sci 16:21759–21774
24. Li ZY, Yu F, Cui L, Chen WM, Wang SX, Zhan P et al (2014) Ligustrazine derivatives. Part 8: design, synthesis, and preliminary biological evaluation of novel ligustrazinyl amides as cardiovascular agents. Med Chem 10:81–89
25. Li GL, Wang PL, Xu X, Lin JX, Chu FH, Song JX et al (2014) Synthesis and protective effect of ligustrazine intermediates against $CoCl_2$-induced neurotoxicity in differentiated PC12 cell. China J Chin Mater Med 39:2679–2683